ORIGINAL ARTICLE

Hsa_circRNA_0000518 facilitates breast cancer development via regulation of the miR-326/FGFR1 axis

Jing Jiang[1,2,3,4,5,6], Hui Lin[1,2,3,4,7], Shenghong Shi[5,6], Ying Hong[5,6], Xianan Bai[5,6] & Xuchen Cao[1,2,3,4] (iD)

1 The First Department of Breast Cancer, Tianjin Medical University Cancer Institute Hospital, National Clinical Research Center for Cancer, Tianjin, China
2 Key Laboratory of Cancer Prevention and Therapy, Tianjin, China
3 Tianjin's Clinical Research Center for Cancer, Tianjin, China
4 Key Laboratory of Breast Cancer Prevention and Therapy, Tianjin Medical University, Ministry of Education, Tianjin, China
5 Department of Breast Surgery, HwaMei Hospital, University of Chinese Academy of Sciences, Ningbo, China
6 Ningbo Institute of Life and Health Industry, University of Chinese Academy of Sciences, Ningbo, China
7 Department of Thyroid and Breast Surgery, Taizhou Hospital of Zhejiang Province Affiliated to WenZhou Medical University, Taizhou, China

*Correspondence
Xuchen Cao, The First Department of Breast Cancer, Tianjin Medical University Cancer Institute Hospital, National Clinical Research Center for Cancer, Huanhu West Road, Hexi District, Tianjin 300060, China.
Email: caoxuchen@tmu.edu.cn
Tel:+86 131 6590 3056
Fax: +86 0574 8387 1172

†These authors contributed equally to this paper.

Abstract

Background: Breast cancer (BC) is a heterogeneous malignant tumor that threatens the health of women worldwide. Hsa_circRNA_0000518 (circ_0000518) has been revealed to be upregulated in BC tissues. However, the role and mechanism of circ_0000518 in BC are indistinct.

Methods: Quantitative real-time polymerase chain reaction (qRT-PCR) was implemented to detect the levels of circ_0000518, microRNA (miR)-326, and fibroblast growth factor receptor 1 (FGFR1) mRNA in BC tissues and cells. Cell counting kit-8 (CCK-8), colony formation, flow cytometry, and transwell assays were executed to estimate BC cell proliferation, cell cycle progression, apoptosis, migration, and invasion. The relationship between circ_0000518 or FGFR1 and miR-326 was verified by dual-luciferase reporter and/or RNA immunoprecipitation (RIP) assays. The role of circ_0000518 in vivo was confirmed by xenograft assay.

Results: Circ_0000518 and FGFR1 were upregulated while miR-326 was down-regulated in BC tissues and cells. Circ_0000518 silencing impeded tumor growth in vivo and induced cell cycle arrest, apoptosis, cured proliferation, colony formation, migration, and invasion of BC cells in vitro. Circ_0000518 regulated FGFR1 expression via competitively binding to miR-326 in BC cells. MiR-326 inhibitor reversed the inhibitory influence of circ_0000518 knockdown on the malignant behaviors of BC cells. FGFR1 overexpression abolished miR-326 mimic-mediated influence on the malignant behaviors of BC cells.

Conclusions: Circ_0000518 facilitated BC development via regulation of the miR-326/FGFR1 axis, suggesting that circ_0000518 might be a promising target for BC treatment.

Introduction

Breast cancer (BC) is a heterogeneous malignant tumor in women worldwide.[1] In 2018, 2.1 million new cases of BC were diagnosed worldwide, accounting for about a quarter of female cancer cases.[2] At present, primary or neo-adjuvant chemotherapy combined with local therapy (surgery or radiotherapy) and postoperative systemic chemotherapy have become accepted strategies for BC treatment.[3] Because of the high frequency of drug resistance, metastasis, and relapse, the prognosis of BC patients has not been overtly improved.[4, 5] Therefore, it is necessary to further our understanding of the molecular mechanism of BC to formulate more effective treatment strategies.

Circular RNAs (circRNAs), a type of non-coding RNA with a covalently closed circular structure, exert vital biological functions through serving as protein decoys or

microRNA (miR) sponges.[6] CircRNA is more stable than its linear counterpart because it can resist RNase R degradation.[7] CircRNAs have been demonstrated to exert a vital role in the development of diverse diseases.[8, 9] For example, circRNA circ_SMC3 has been reported to accelerate the tumorigenesis of gastric cancer.[10] We analyzed high-throughput circRNA microarray data (GSE101123 database) and found that circ_0000518 was a differentially expressed circRNA in BC. Hsa_circRNA_0000518 (circ_0000518) is formed by the reverse splicing of the ribonuclease P RNA component H1 (RPPH1) gene, and its length is 150 bp. At present, the role of circ_0000518 in BC is unknown.

MiRs are short non-coding RNAs (about 19–25 nucleotides) that exert an important role in cellular processes for normal development.[11] Increasing evidence has indicated that miRs are related to the advancement of various tumors.[12] MiR-326 has been revealed to take part in embryonic development, oncogenesis, chemotherapy resistance, immunomodulation, and cell invasion.[13] MiR-326 has also been identified as a tumor suppressor in a range of tumors, such as papillary thyroid cancer[14] and oral squamous cell cancer,[15] as well as being associated with BC development. However, the mechanism by which miR-326 modulates the advancement of BC has so far not been clearly explained.

Fibroblast growth factor receptor 1 (FGFR1) is a member of the FGFR family, which activates PI3K/AKT signaling and MAPK signaling via acting as a receptor for tyrosine kinase.[16] In gastric cancer, FGFR1 overexpression has been found to contribute to peritoneal dissemination.[17] Moreover, FGFR1 has been demonstrated to facilitate lung cancer cell metastasis and epithelial-mesenchymal transition.[18] FGFR1 signaling has been reported as a vital pathway to drive BC metastasis to the lungs.[19] However, the mechanism of FGFR1 signaling involved in BC progression has not been fully elucidated.

Herein, we discovered that circ_0000518 plays a carcinogenic role in BC, and moreover, was able to facilitate BC progression via regulation of the miR-326/FGFR1 axis.

Methods

Patient-derived samples

Clinical BC tissue samples were collected, including BC tissues and paracarcinoma tissues, from BC patients who accepted surgery in Tianjin Medical University Cancer Institute Hospital. The BC patients who underwent radiotherapy or chemotherapy were excluded in terms of the inclusion criteria. Written informed consents were provided by all enrolled patients. The research was ratified by the Ethics Committee of Tianjin Medical University Cancer Institute Hospital.

Cell culture and transfection

Human normal breast cell line MCF-10A and BC cell lines MCF-7 and MDA-MB-468 were acquired from American Type Culture Collection (Manassas, VA, USA). MCF-10A cells were cultured in MEBM BulletKit (Lonza, Basel, Switzerland). MCF-7 and MDA-MB-468 cells were cultured in Dulbecco's modified Eagle's medium (DMEM, Invitrogen, Sigma, Louis, Missouri, MO, USA) supplemented with fetal bovine serum (FBS, 10%, Sigma), streptomycin (100 μg/mL, Sigma), and penicillin (100 U/mL, Sigma). These cells were kept in a moist atmosphere with 5% CO_2 at 37°C.

Small interference (si) RNA targeting circ_0000518 (si-circ_0000518) and corresponding control (si-NC), as well as miR-326 mimic and inhibitor (miR-326 and anti-miR-326) and their matching negative controls (miR-NC and anti-miR-NC), were obtained from GenePharma (Shanghai, China). The overexpression vectors of FGFR1 (pcDNA-FGFR1) and circ_0000518 (circ_0000518) were established via cloning the full-length sequence of FGFR1 or circ_0000518 into the pcDNA3.1 vector (pcDNA-NC) (Invitrogen, Carlsbad, CA, USA) or pcD-ciR (Geneseed Biotech Co., Ltd., Guangzhou, China) (Vector). BC cells (MCF-7 and MDA-MB-468) were transfected with oligo-nucleotides or vectors using Lipofectamine 3000 reagent (Life Technologies, Grand Island, NY, USA).

Quantitative real-time polymerase chain reaction (qRT-PCR)

Total RNA was extracted from tissue samples and cells with RNAiso Plus (Takara, Dalian, China). Next, the complementary DNA was synthesized with the PrimeScript RT reagent Master Mix (Takara) or Mir-X miRNA First-Strand Synthesis Kit (Takara). QRT-PCR was executed by using a Light Cycler 480 II Real-Time PCR System (Roche, Basel, Switzerland) with the SYBR Premix Ex Taq kit (Takara). The $2^{-\Delta\Delta Ct}$ method was utilized to calculate the expression of circ_0000518, miR-326, and FGFR1, and glyceraldehyde-3-phosphate dehydrogenase (GAPDH) or U6 small nuclear RNA (snRNA) was used as the control. The primers were used as below: circ_0000518: (F:5′-AGGTGAGTTCCCAGAGAACGG-3′ and R:5′-AGTGG AGTGACAGGACGCA-3′); GAPDH: (F:5′-GACTCCACT CACGGCAAATTCA-3′ and R:5′-TCGCTCCTGGAAGA TGGTGAT-3′); miR-326: (F:5′-CCTCTGGGCCCTTCCTC CAG-3′ and R:5′-GCTGTCAACGATACGCTACCTA-3′); U6 snRNA (F:5′-GCTCGCTTCGGCAGCACA-3′ and R:5′-GAGGTATTCGCACCAGAGGA-3′); FGFR1: (F:5′-CCC

GTAGCTCCATATTGGACA-3′ and R:5′-TTTGCCATTT
TTCAACCAGCG -3′).

Cell proliferation assay

After transfection with oligonucleotides or vectors, the BC
cells (5×10^3 cells/well) were cultured for 24, 48, or
72 hours under the right conditions. Next, 10 μL cell cou-
nting kit-8 (CCK-8) reagent (Dojindo, Tokyo, Japan) was
complemented into each well following the manufacturer's
protocol. Thereafter, the absorbance at 450 nm was mea-
sured with the microplate absorbance reader (Bio-Rad,
Hercules, CA, USA).

Cell colony formation assay

The transfected BC cells (5×10^3) were seeded in a six-well
plate with DMEM and cultured for 14 days. Subsequently,
the cells were fixed with paraformaldehyde (4%) and sta-
ined with crystal violet (0.5%, Beyotime, Shanghai, China).
After washing with phosphate buffer solution (PBS), the
colonies (>50 cells) were counted and photographed via
light microscope (Olympus, Tokyo, Japan).

Cell cycle and apoptosis analysis

For cell cycle assay, the BC cells were transfected with
appointed oligonucleotides or vectors. After culture for
48 hours, the cells were treated with propidium iodide
(PI) (50 μg/mL, Sigma) solution containing sodium citrate
(0.1%) and Triton X-100 (0.1%). For cell apoptosis assay,
the transfected BC cells were treated with the FITC-
Annexin V Apoptosis Detection Kit (Dojindo). Cell cycle
and apoptosis were estimated with a FACScalibur flow
cytometer (BD Biosciences, San Jose, CA, USA).

Cell migration and invasion analysis

The migration capacity of the transfected BC cells was
evaluated with an 8 μm pore membrane filter (Costar,
Cambridge, MA, USA). In brief, the DMEM (serum-free)
containing BC cells (1×10^5 cells) was added to the upper
chamber. The lower chamber was supplemented with the
DMEM containing 10% FBS. After incubation for 24 hours,
the cells on the lower surface of the membrane were fixed
with paraformaldehyde (4%) and stained with crystal violet
(0.5%, Beyotime). Thereafter, the cells were visualized and
counted with a light microscope (Olympus) at 100 ×
magnification. The cell invasion test was performed in the
same way as the migration test, except that the 8 μm pore
membrane filter used in the cell invasion test was pre-
coated with Matrigel (BD Biosciences).

Dual-luciferase reporter assay

The binding sites between circ_0000518 or FGFR1 and
miR-326 were predicted by using the circInteractome or
targetscan databases. The sequences of wild-type
circ_0000518 (circ_0000518-WT), mutant circ_0000518
(circ_0000518-MUT), wild-type 3′ untranslated regions
(UTR) of FGFR1 (FGFR1 3′UTR-WT), and mutant 3′UTR
of FGFR1 (FGFR1 3′UTR-MUT) were inserted into the
pmirGLO luciferase vectors (GeneCreat, Wuhan, China) to
construct the luciferase reporters, respectively. Then, the
luciferase reporters were cotransfected into BC cells with
miR-NC or miR-326. The luciferase intensities were deter-
mined with the luciferase reporter assay kit (Promega,
Madison, WI, USA) by normalizing the firefly lumines-
cence to Renilla luminescence.

RNA immunoprecipitation (RIP) assay

The specific binding circ_0000518 and miR-326 were veri-
fied with a Magna RIP kit (Millipore, Bedford, MA, USA).
In short, BC cells were lysed in complete RNA lysis buffer.
Thereafter, the lysate was incubated with RIP immunopre-
cipitation buffer including protein A/G sepharose beads
conjugated with IgG antibody (ab109489, 1:100, Abcam,
Cambridge, MA, USA) or Ago-2 antibody (ab186733, 1:50,
Abcam). The immunoprecipitated RNA was extracted
using the RNeasy Mini Kit (Qiagen). QRT-PCR was uti-
lized to analyze the enrichment of circ_0000518 and miR-
326 in the immunoprecipitated RNA.

Western blotting

Total protein was extracted from tissue samples and cells
with RIPA lysis buffer containing protease inhibitor
(Beyotime). Total protein was separated by using sodium
dodecyl sulfate-polyacrylamide gel electrophoresis (SDS-
PAGE). Thereafter, the separated proteins were transferred
to polyvinylidene difluoride (PVDF) membranes
(Beyotime), and the membranes were blocked with tris
buffered saline tween buffer with 5% skim milk. The mem-
branes were then incubated with primary antibodies,
including anti-FGFR1 (ab76464, 1:500, Abcam) and anti-
GAPDH (ab9484, 1:1000, Abcam). GAPDH was deemed
as a loading control. Next, the membranes were incubated
with the secondary antibody (ab6721, 1:5000, Abcam). The
immunoblots were visualized with enhanced chemilumi-
nescence solution (Beyotime).

Xenograft assay

Circ_0000518 short hairpin RNA (sh-circ_0000518) and
matching control (sh-NC) were purchased from

GenePharma. The circ_0000518-knockdown MCF-7 cells were constructed through infecting with the hU6-MCS-CMV-Puromycin lentiviral vectors with sh-circ_0000518. The MCF-7 cells (1×10^7 cells/0.2 mL PBS) carrying sh-circ_0000518 or sh-NC were subcutaneously injected into the right flank of 10 BALB/c nude mice (5-week-old, Experimental Animal Center, Shanghai, China) (five mice/group). All nude mice were fed under specific pathogen free conditions. The mice were sacrificed by cervical dislocation under 5% isoflurane to acquire their tumor tissues after injection after 27 days. Tumor volume was measured every four days using a caliper. Tumor volume was calculated in light of the following equation: Volume = (length $\times$ width^2)/2. The protocols of tumor formation experiments were approved by the Animal Ethics Committee of Tianjin Medical University Cancer Institute Hospital.

Statistical analysis

All in vitro experiments in this study were repeated at least three times. Statistical analysis was implemented with GraphPad Prism 6 software (GraphPad, San Diego, CA, USA). Data are shown as mean ± standard deviation. The normal distribution of the data was determined with a Kolmogorov-Smirnov test. Differences were deemed significant if $P < 0.05$. The differences between two groups were determined with Student's t-test, and three or more groups were estimated by using one-way variance analysis (ANOVA) with hoc post Turkey test. The homogeneity of the variances was analyzed with the F-test.

Results

Microarray data of circRNAs differentially expressed in BC

To identify differentially expressed circRNAs in BC, we analyzed high-throughput circRNA microarray data (GSE101123 database). We selected 20 circRNAs that were significantly upregulated or downregulated in BC tissues and then plotted a heat map (Fig 1). Among 20 differentially expressed circRNAs, we selected five circRNAs (hsa_circRNA_001846, hsa_circRNA_000518, hsa_circRNA_002172, hsa_circRNA_002144, and hsa_circRNA_000166) for preliminary experiment. QRT-PCR showed that hsa_circRNA_001846, hsa_circRNA_000518, and hsa_circRNA_000166 were significantly upregulated in BC tissue samples (10 random samples). We selected hsa_circRNA_000518, which had a relatively larger expression change, as the research object (Fig S1).
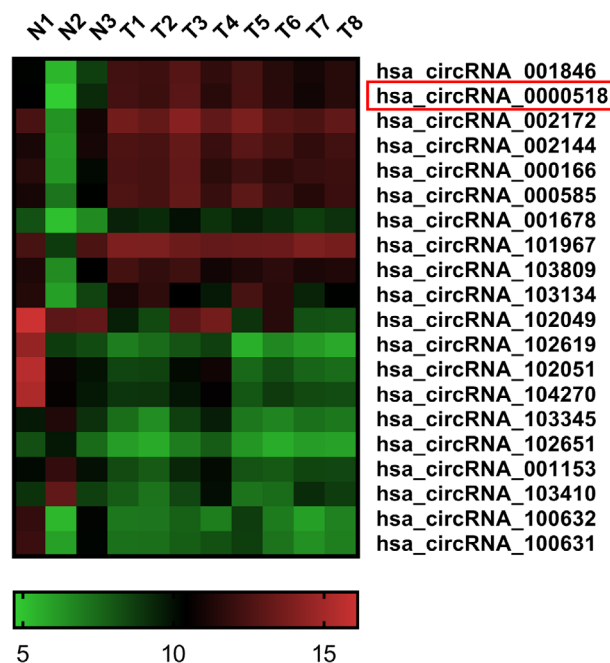

Figure 1 Microarray data of 20 differentially expressed circRNAs in BC. Heat map exhibiting 20 differentially expressed circRNAs (GSE101123 database).

Circ_0000518 accelerated the malignancy of BC cells

To explore the biological function of circ_0000518 in BC, we examined the levels of circ_0000518 in 35 paired BC tissues and para-carcinoma tissues. QRT-PCR manifested that circ_0000518 expression was increased in BC tissues in contrast to the paracarcinoma tissues (Fig 2a). Circ_0000518 expression was also elevated in BC cell lines (MCF-7 and MDA-MB-468) relative to the MCF-10A cell line (Fig 2b). The knockdown efficiency of circ_0000518 is shown in Fig 2c. Subsequently, CCK-8 assay indicated that circ_0000518 downregulation could curb the proliferation of MCF-7 and MDA-MB-468 cells (Fig 2d,e). Cell colony formation assay manifested that the colony number of MCF-7 and MDA-MB-468 cells was decreased by circ_0000518 inhibition (Fig 2f). Flow cytometry assay showed that silenced circ_0000518 expression arrested cell cycle progression and induced cell apoptosis in MCF-7 and MDA-MB-468 cells (Fig 2g–i). Transwell assay revealed that circ_0000518 silencing repressed cell migration and invasion in MCF-7 and MDA-MB-468 cells (Fig 2j,k). We also explored the influence of circ_0000518 overexpression on the malignancy of BC cells. The overexpression efficiency of circ_0000518 is shown in Fig S2A. Also, the overexpression of circ_0000518 reduced cell apoptosis and accelerated cell proliferation, colony formation, cell cycle progression, migration, and invasion in BC cells (Fig S2B–I). These
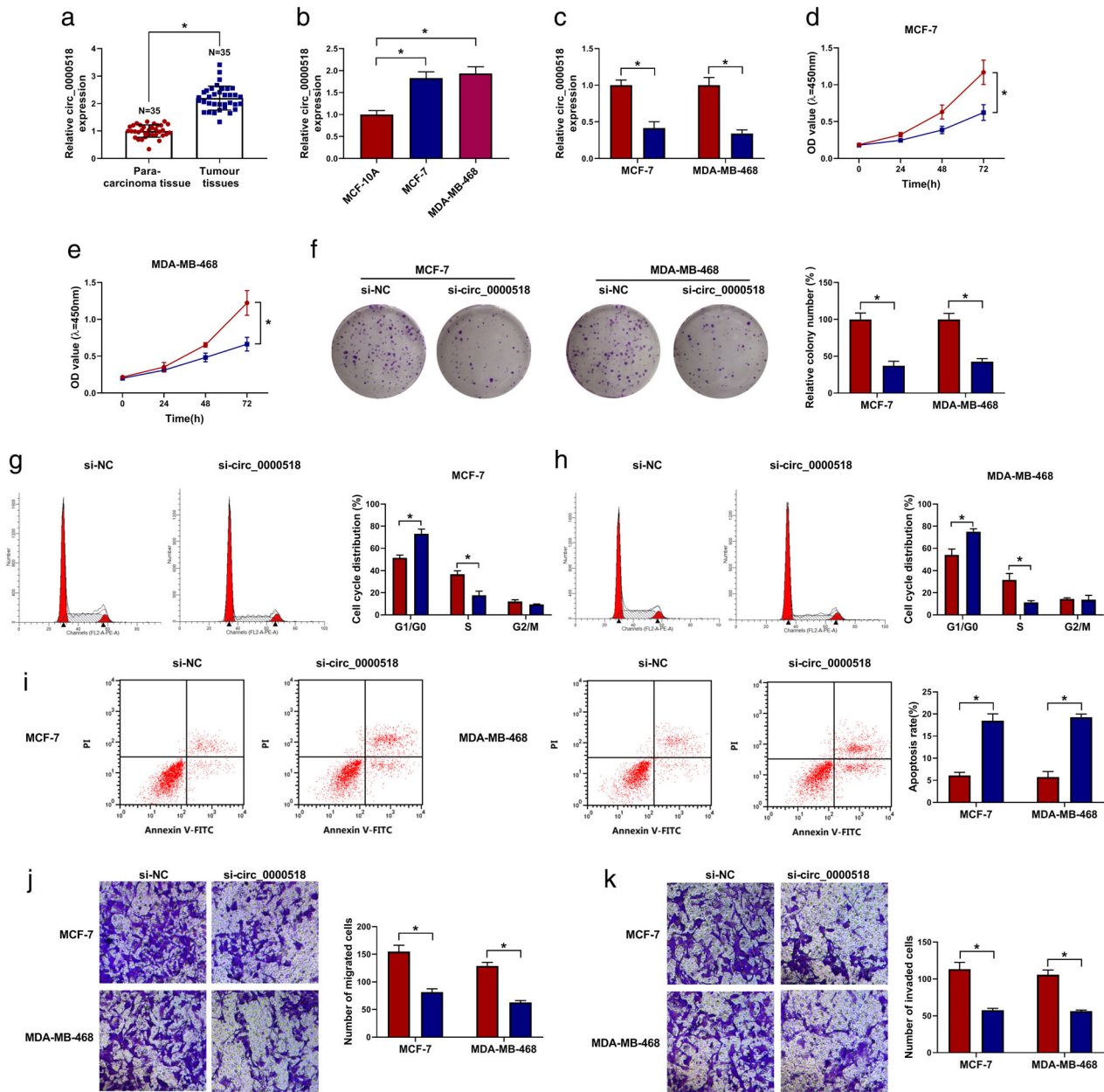
Figure 2 Effects of circ_0000518 knockdown on cell proliferation, colony formation, cell cycle progression, apoptosis, migration, and invasion in BC cells. (**a** and **b**) QRT-PCR was performed to examine the expression of circ_0000518 in 35 paired BC tissues and para-carcinoma tissues, as well as BC cell lines (MCF-7 and MDA-MB-468) and MCF-10A cell line. (**c–k**) The proliferation, colony formation, cell cycle progression, apoptosis, migration, and invasion of MCF-7 and MDA-MB-468 cells after si-circ_0000518 or si-NC transfection were determined with CCK-8, colony formation, flow cytometry, or transwell assays. The experiments were repeated three times. Data are shown as mean ± standard deviation. *$P < 0.05$. (**c**) (▨) si-NC and (▨) si-circ_0000518. (**d**) MCF-7 (—●—) si-NC and (—■—) si-circ_0000518. (**e**) MDA-MB-468 (—●—) si-NC and (—■—) si-circ_0000518. (**f**) (▨) si-NC and (▨) si-circ_0000518. (**g**) si-NC (▨) si-NC, (▨) si-NC, and (▨) si-circ_0000518 and si-circ_0000518 (▨) si-NC, (▨) si-NC, and (▨) si-circ_0000518. MCF-7 (▨) si-NC and (▨) si-circ_0000518. (**h**) si-NC (▨) si-NC, (▨) si-NC, and (▨) si-circ_0000518 and si-circ_0000518 (▨) si-NC, (▨) si-NC, and (▨) si-circ_0000518. MDA-MB-468 (▨) si-NC and (▨) si-circ_0000518. (**i**) (▨) si-NC and (▨) si-circ_0000518. (**j**) (▨) si-NC and (▨) si-circ_0000518. (**k**) (▨) si-NC and (▨) si-circ_0000518.

finding manifested that circ_0000518 facilitated the malignant behavior of BC cells.

Circ_0000518 identified as a sponge for miR-326, which targeted FGFR1 in BC cells

Subsequently, we further explored the molecular mechanism of circ_0000518 in BC. We found that miR-326 had the potential binding sites for circ_0000518 through using the circInteractome database. Targetscan database showed that miR-326 had complementary sites to FGFR1 (Fig 3a). Dual-luciferase reporter assay revealed that miR-326 elevation inhibited the luciferase intensity of the luciferase reporters with circ_0000518-WT in MCF-7 and MDA-MB-468 cells compared to the control miR-NC, while there was no overt change in the luciferase reporters with circ_0000518-MUT (Fig 3b,c). RIP assay exhibited that circ_0000518 and miR-326 were preferentially enriched in Ago2-containing complexes compared to the control group (Fig 3d,e). Also, the luciferase activity of the FGFR1 3′UTR-WT reporter was suppressed by miR-326 mimic in MCF-7 and MDA-MB-468 cells, but the luciferase activity of the FGFR1 3′UTR-MUT reporter did not change (Fig 3f,g). Furthermore, miR-326 expression was decreased in BC tissues and cell lines in comparison to their matching controls (Fig 3h,i). Inversely, FGFR1 mRNA and protein levels were elevated in BC tissues and cell lines (Fig 3j–m). The expression of miR-326 and circ_0000518 or FGFR1 mRNA in BC tissues had a negative correlation (Fig 3n,o). However, the expression of FGFR1 mRNA was positively correlated with circ_0000518 in BC cells (Fig 3p). These results indicated that circ_0000518 served as a sponge for miR-326, which targeted FGFR1 in BC cells.

Circ_0000518 regulated FGFR1 expression through competitively binding to miR-326 in BC cells

Based on the above findings, we further investigated whether circ_0000518 acted as a competing endogenous RNA (ceRNA) in BC cells. The results showed that miR-326 expression was markedly reduced in MCF-7 and MDA-MB-468 cells after transfection with anti-miR-326 compared to the control anti-miR-NC (Fig 4a). Furthermore, circ_0000518 silencing downregulated the levels of FGFR1 mRNA and protein in MCF-7 and MDA-MB-468 cells, but this trend was recovered after anti-miR-326 transfection (Fig 4b,c). These data indicated that circ_0000518 regulated FGFR1 expression through sponging miR-326 in BC cells.

MiR-326 inhibitor abolished circ_0000518 silencing-mediated influence on the malignancy of BC cells

Given that circ_0000518 acted as a sponge for miR-326, we further surveyed the mechanism between circ_0000518 and miR-326 in BC progression. The results exhibited that miR-326 expression was increased in circ_0000518-silenced MCF-7 and MDA-MB-468 cells, while this trend was reversed after miR-326 inhibitor transfection (Fig 5a). Furthermore, the inhibitory influence of circ_0000518 knockdown on proliferation, colony formation, and cell cycle progression of MCF-7 and MDA-MB-468 cells was overturned by miR-326 inhibition (Fig 5b–f). Moreover, the elevation of the apoptotic rate of MCF-7 and MDA-MB-468 cells caused by circ_0000518 inhibition was recovered after miR-326 silencing (Fig 5g). Also, decreased miR-326 expression overturned the repression of migration and invasion of MCF-7 and MDA-MB-468 cells mediated by circ_0000518 inhibition (Fig 5h,i). Taken together, these data indicated that circ_0000518 modulated BC progression via sponging miR-326.

FGFR1 overexpression recovered miR-326 mimic-mediated impacts on the malignancy of BC cells

Considering that FGFR1 was a downstream target for miR-326 in BC, we explored whether miR-326 played its role through FGFR1. We discovered that miR-326 mimic inhibited the levels of FGFR1 mRNA and protein in MCF-7 and MDA-MB-468 cells, while this influence was partly reversed after pcDNA-FGFR1 transfection (Fig 6a–c). Furthermore, miR-326 mimic cured cell proliferation, colony formation, and cell cycle progression in MCF-7 and MDA-MB-468 cells, while this impact was overturned by FGFR1 overexpression (Fig 6d–h). Also, miR-326 mimic elevated the apoptotic rate of MCF-7 and MDA-MB-468 cells, but this tendency was overturned after FGFR1 upregulation (Fig 6i). Additionally, enhanced FGFR1 expression abolished the repressive impact of miR-326 elevation on migration and invasion of MCF-7 and MDA-MB-468 cells (Fig 6j,k). Collectively, these results indicated that miR-326 played its role through targeting FGFR1 in BC cells.

Circ_0000518 inhibition curbed tumor growth in vivo

Knowing that circ_0000518 played a promoting role in BC cells in vitro, we further confirmed the role of circ_0000518 in BC in vivo through xenograft assay. We observed that tumor volume and weight were repressed
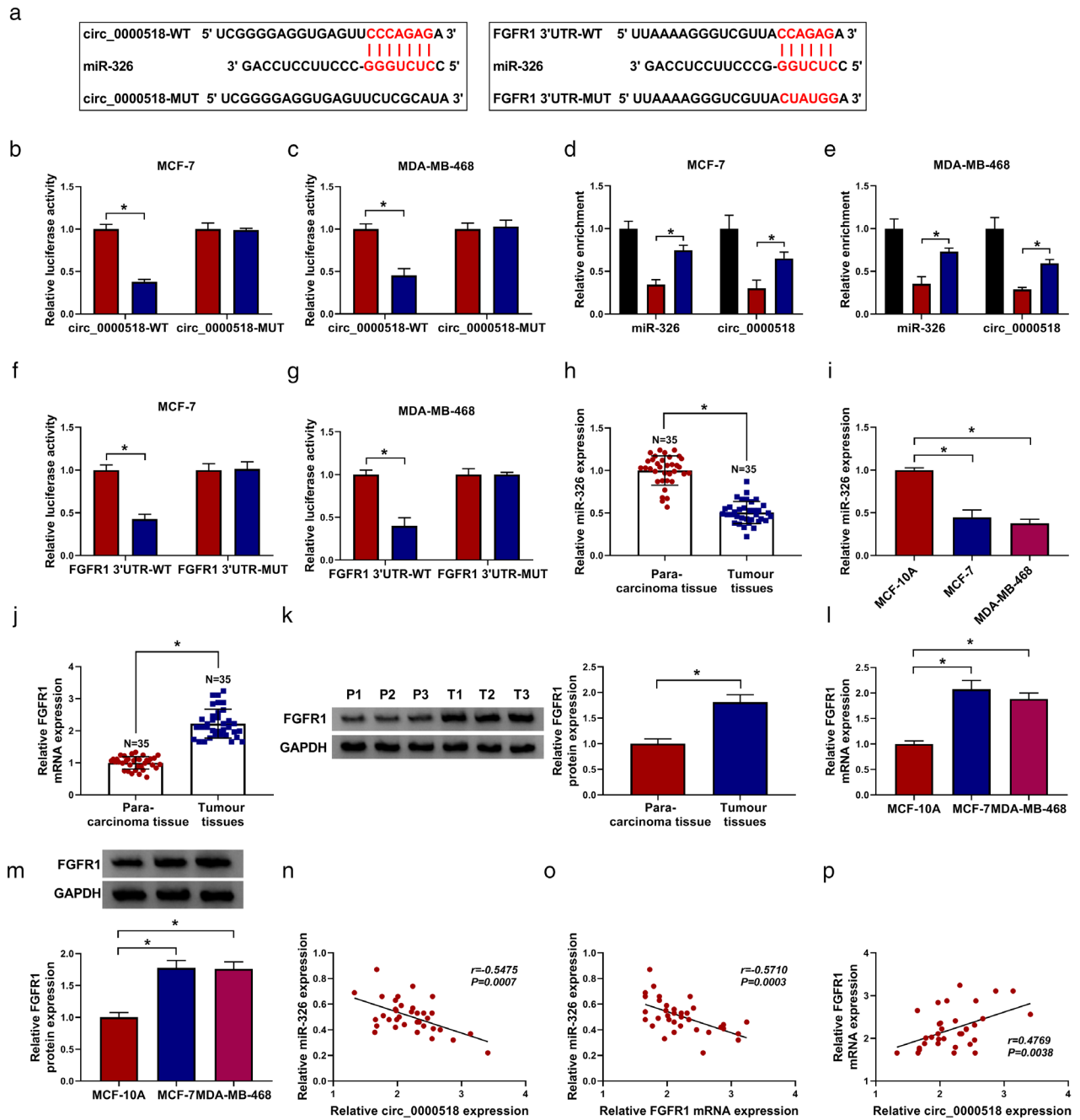
Figure 3 Circ_0000518 acted as a sponge for miR-326, which targeted FGFR1 in BC cells. (**a**) The binding sites between miR-326 and circ_0000518 or FGFR1 were predicted with circInteractome or targetscan databases. (**b** and **c**) Dual-luciferase reporter assay was conducted to evaluate the luciferase activity of luciferase reporters with circ_0000518-WT or circ_0000518-MUT in MCF-7 and MDA-MB-468 cells transfected with miR-326 or miR-NC. (**d** and **e**) After RIP assay, the enrichment of miR-326 and circ_0000518 was examined using qRT-PCR. (**f** and **g**) Dual-luciferase reporter assay revealed the luciferase activities of the FGFR1 3′UTR-WT and FGFR1 3′UTR-MUT reporters in MCF-7 and MDA-MB-468 cells transfected with miR-326 or miR-NC. (**h** and **i**) Expression levels of miR-326 in BC tissues and para-carcinoma tissues, as well as BC (MCF-7 and MDA-MB-468) and MCF-10A cells, were assessed by qRT-PCR. (**j**–**m**) The mRNA and protein levels of FGFR1 in BC tissues and para-carcinoma tissues, as well as BC (MCF-7 and MDA-MB-468) and MCF-10A cells, were detected by qRT-PCR or western blotting. (**n**–**p**) The correlation among miR-326, circ_0000518, and FGFR1 in BC tissues was determined via Pearson's correlation analysis. The experiments were repeated three times. Data are shown as mean ± standard deviation. *$P < 0.05$. (**b**) MCF-7 (■) miR-NC and (■) miR-326. (**c**) MDA-MB-468 (■) miR-NC and (■) miR-326. (**d**) MCF-7 (■) input, (■) anti-IgG, and (■) anti-Ago2. (**e**) MDA-MB-468 (■) anti-IgG, (■) input, and (■) anti-Ago2. (**f**) MCF-7 (■) miR-NC and (■) miR-326. (**g**) MDA-MB-468 (■) miR-NC and (■) miR-326.
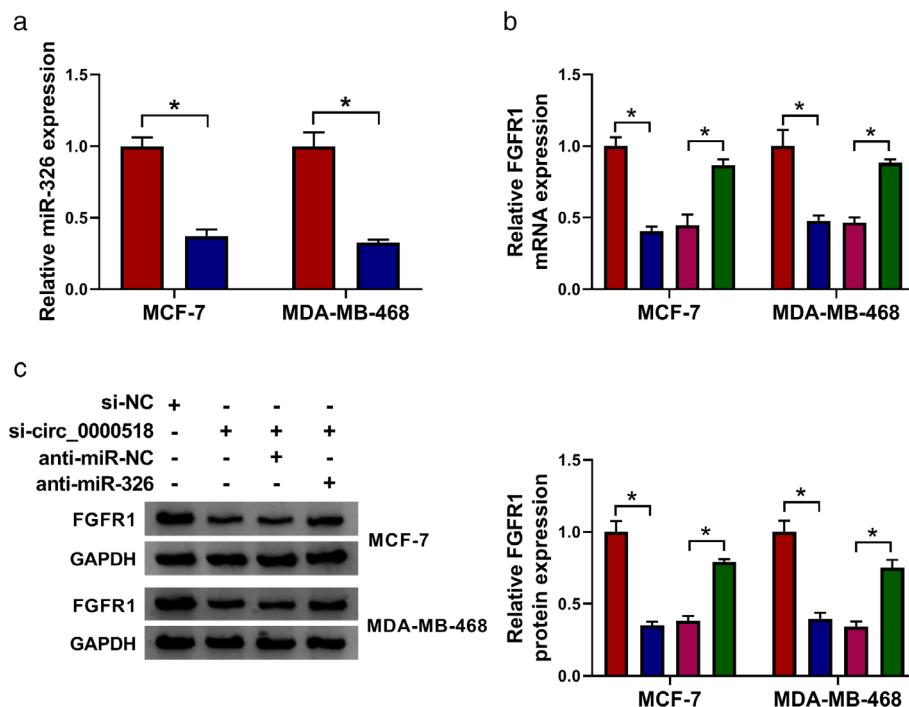
a

b

c

Figure 4 Circ_0000518 regulated FGFR1 expression through sponging miR-326 in BC cells. (**a**) QRT-PCR was carried out to assess the levels of miR-326 in MCF-7 and MDA-MB-468 cells after anti-miR-NC or anti-miR-326 transfection. (**b** and **c**) The levels of FGFR1 mRNA and protein in MCF-7 and MDA-MB-468 cells transfected with si-NC, si-circ_0000518, si-circ_0000518+anti-miR-NC, or si-circ_0000518+anti-miR-326 were examined via qRT-PCR or western blotting. The experiments were repeated 3 times. Data are shown as mean ± standard deviation. *$P < 0.05$. (**a**) (■) Anti-miR-NC and (■) anti-miR-326. (**b**) (■) si-NC, (■) si-circ_0000518, (■) si-circ_0000518 + anti-miR-NC, and (■) si-circ_0000518 + anti-miR-326. (**c**) (■) si-NC, (■) si-circ_0000518, (■) si-circ_0000518 + anti-miR-NC, and (■) si-circ_0000518 + anti-miR-326.

and decreased in the sh-circ_0000518 group relative to the sh-NC group (Fig 7a,b). Also, circ_0000518 expression was decreased while miR-326 expression was increased in mice tumor tissues of the sh-circ_0000518 group in comparison to the sh-NC group (Fig 7c,d). Moreover, the levels of FGFR1 mRNA and protein were decreased in the sh-circ_0000518 group (Fig 7e,f). These data manifested that circ_0000518 silencing could decrease BC growth in vivo.

Discussion

Emerging studies have demonstrated the vital roles of circRNAs in tumor development and progression.[20] Some circRNAs have been verified as latent therapeutic targets and novel biomarkers in a series of diseases, including tumors.[21] A previous report revealed that circRNA circ_KDM4C moderated doxorubicin resistance and impeded tumor growth in BC through increasing PBLD expression by sponging miR-548p.[22] Also, circRNA hsa_circ_0009362,[23] circRNA circ_TFF1,[24] and circRNA circACAP2[25] contributed to the advancement of BC. In the current study, circ_0000518 level was elevated in BC tissues and cells. Circ_0000518 silencing reduced tumor growth in vivo and facilitated cell cycle arrest, apoptosis, impeded proliferation, colony formation, migration, and invasion of BC cells in vitro. To the best of our knowledge, our research is the first to clarify the biological function of circ_0000518, and therefore we concluded that circ_0000518 exerted a carcinogenic role in BC.

Increasing evidence has demonstrated that circRNAs serve as ceRNAs taking part in the occurrence and progression of tumors. Recent research has shown that circRNA circ_SEPT9 facilitated triple-negative BC carcinogenesis and advancement through activation of the LIF/STAT3 pathway via sponging miR-637.[26] Herein, we discovered that circ_0000518 served as a sponge for miR-326 in BC cells. Previous studies have demonstrated that miR-326 exerted a repressive role in diverse cancers.[27–30] Ghaemi *et al.* revealed that miR-326 curbed BC progression via inactivation of the ErbB/PI3K pathway.[31] Du *et al.* indicated that miR-326 could impede invasion, migration, and proliferation of BC cells through targeting SOX12.[32] Another study uncovered that miR-326 expression was repressed by circRNA circ_TFF1, which contributed to BC development.[24] Liang *et al.* claimed that miR-326 mimic could elevate sensitivity of BC cells to doxorubicin through regulating MRP1 expression.[33] In the research, miR-326 expression was decreased in BC tissues and cells. Also, miR-326 inhibitor reserved circ_0000518 silencing-mediated impacts on proliferation, colony formation, cell cycle progression, apoptosis, migration, and invasion of BC cells. Therefore, these data indicated that circ_0000518 regulated BC progression via sponging miR-326.

FGFR1 has been demonstrated as an oncogene in a series of cancers.[17, 18] C11, an inhibitor of FGFR1, could curb angiogenesis and metastasis of BC.[34] Previous research revealed that FGFR1 promoted resistance to endocrine therapy and acted as a possible target for BC.[35] One
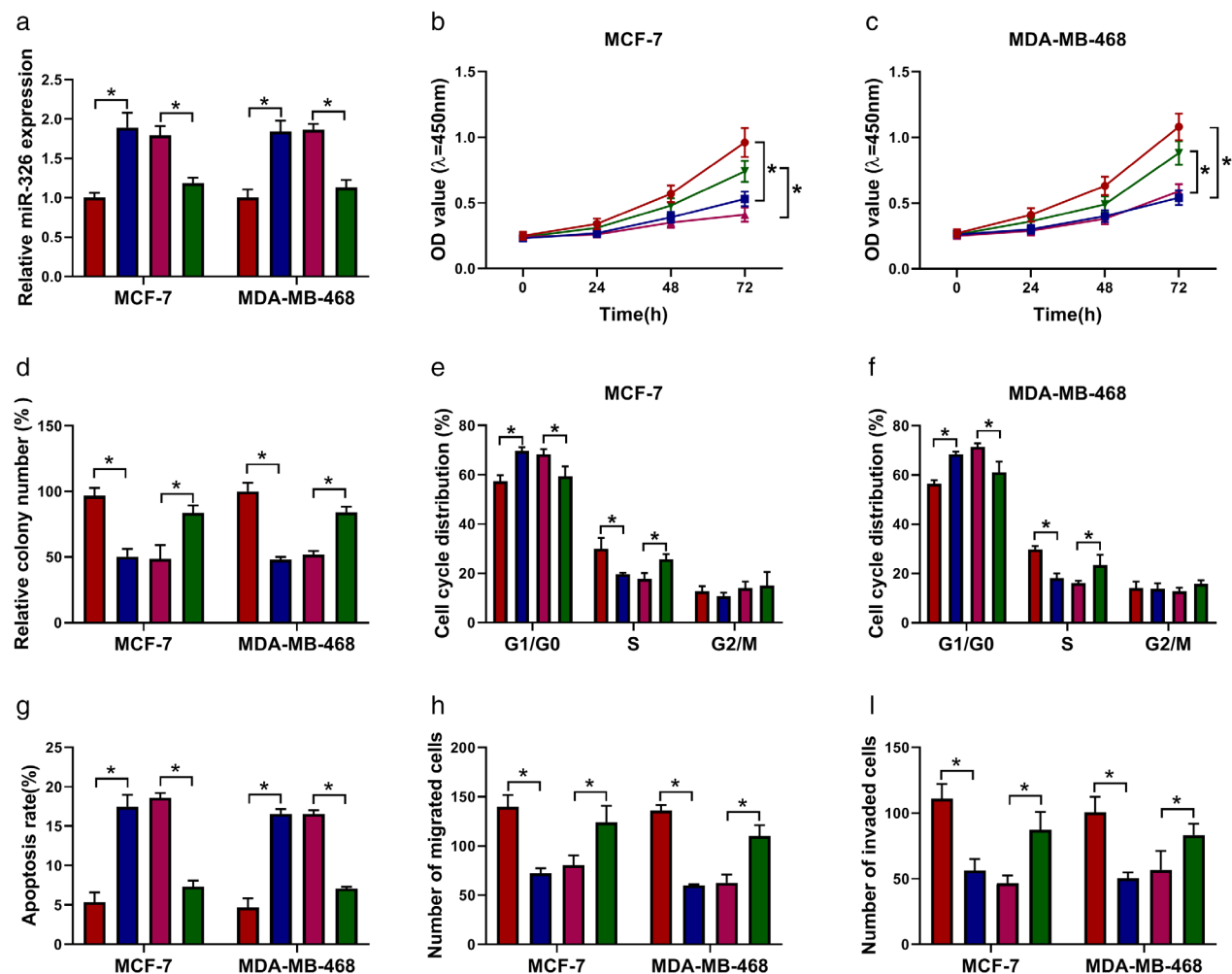
Figure 5 Circ_0000518 regulated BC progression via sponging miR-326. (**a**–**i**) MCF-7 and MDA-MB-468 cells were transfected with si-NC, si-circ_0000518, si-circ_0000518 + anti-miR-NC, or si-circ_0000518 + anti-miR-326. (**a**) Expression levels of miR-326 in MCF-7 and MDA-MB-468 cells were detected through qRT-PCR. (**b**–**i**) The proliferation, colony formation, cell cycle progression, apoptosis, migration, and invasion of MCF-7 and MDA-MB-468 cells were evaluated through CCK-8, colony formation, flow cytometry, or transwell assays. The experiments were repeated three times. Data are shown as mean ± standard deviation. *$P < 0.05$. (**a**) (■) si-NC, (■) si-circ_0000518, (■) si-circ_0000518 + anti-miR-NC, and (■) si-circ_0000518 + anti-miR-326. (**b**) MCF-7 (—●—) si-NC, (—■—) si-circ_0000518, (—▲—) si-circ_0000518 + anti-miR-NC, and (—▼—) si-circ_0000518 + anti-miR-326. (**c**) MDA-MB-468 (—●—) si-NC, (—■—) si-circ_0000518, (—▲—) si-circ_0000518 + anti-miR-NC, and (—▼—) si-circ_0000518 + anti-miR-326. (**d**) (■) si-NC, (■) si-circ_0000518, (■) si-circ_0000518 + anti-miR-NC, and (■) si-circ_0000518 + anti-miR-326. (**e**) MCF-7 (■) si-NC, (■) si-circ_0000518, (■) si-circ_0000518 + anti-miR-NC, and (■) si-circ_0000518+anti-miR-326. (**f**) MDA-MB-468 (■) si-NC, (■) si-circ_0000518, (■) si-circ_0000518 + anti-miR-NC, and (■) si-circ_0000518 + anti-miR-326. (**g**) (■) si-NC, (■) si-circ_0000518, (■) si-circ_0000518 + anti-miR-NC, and (■) si-circ_0000518 + anti-miR-326. (**h**) (■) si-NC, (■) si-circ_0000518, (■) si-circ_0000518 + anti-miR-NC, and (■) si-circ_0000518 + anti-miR-326. (**i**) (■) si-NC, (■) si-circ_0000518, (■) si-circ_0000518 + anti-miR-NC, and (■) si-circ_0000518 + anti-miR-326.

report uncovered that FGFR1 expression was inhibited by miR-361-5p, which impeded BC cell invasion, proliferation, and glycolysis.[36] Golfmann *et al.* unraveled that targeting both FGFR1 and VEGFR1 had a synergistic therapeutic effect in FGFR1/VEGFR1-positive BC patients.[37] In the present research, we revealed that FGFR1 was a target for miR-326 in BC. Moreover, circ_0000518 regulated FGFR1 expression via sponging miR-326. FGFR1

overexpression abolished the impact of miR-326 mimic on proliferation, colony formation, cell cycle progression, apoptosis, migration, and invasion of BC cells. Therefore, we concluded that circ_0000518 regulated BC progression via modulating the miR-326/FGFR1 axis.

In conclusion, our research showed the critical role of circ_0000518 in BC. Circ_0000518 accelerated BC progression via elevating FGFR1 expression by sponging miR-326.
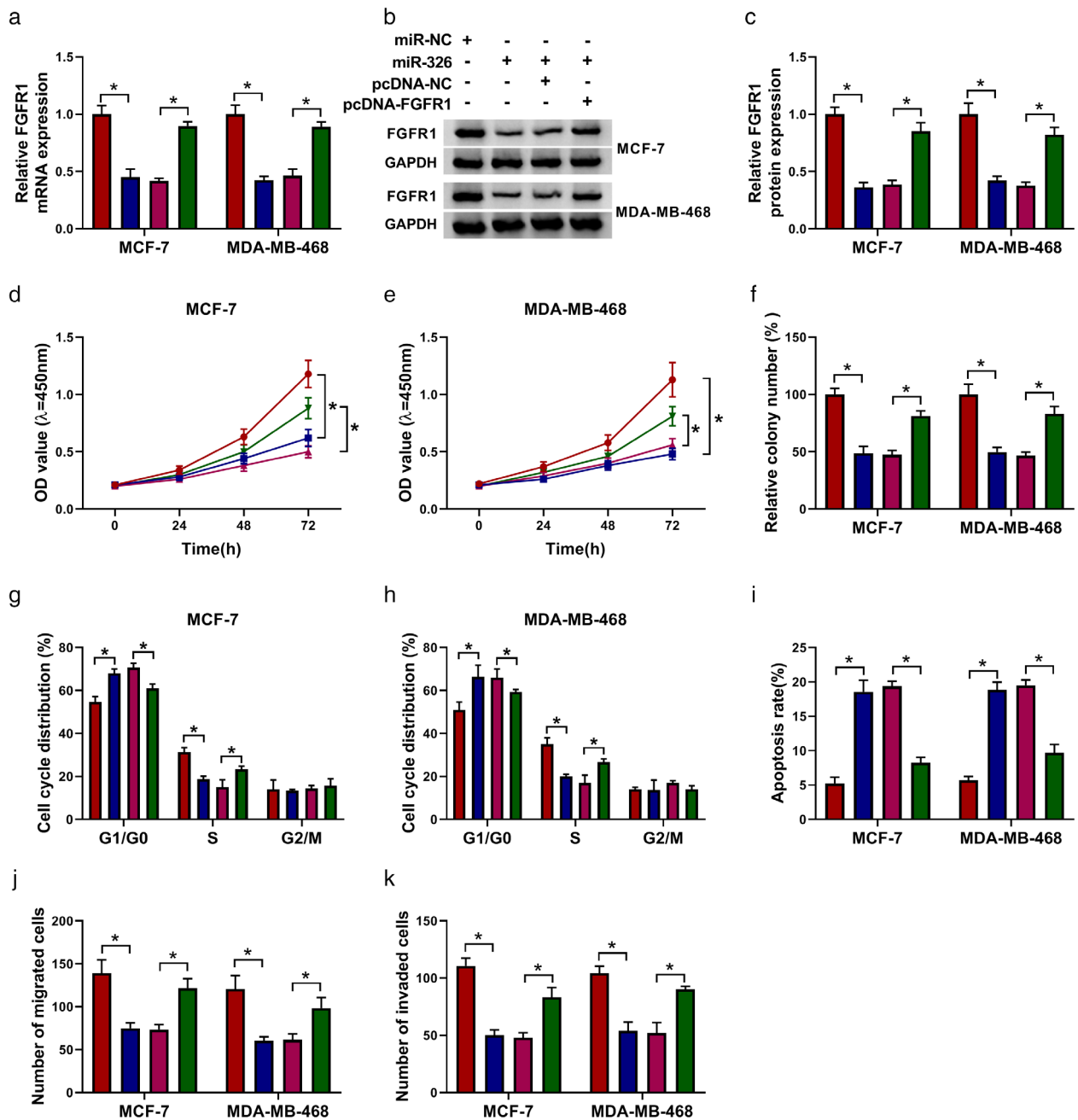
Figure 6 MiR-326 regulated BC advancement via targeting FGFR1 in BC cells. (**a–k**) MCF-7 and MDA-MB-468 cells were transfected with miR-NC, miR-326, miR-326 + pcDNA-NC, or miR-326 + pcDNA-FGFR1. (**a–c**) The mRNA and protein level of FGFR1 in MCF-7 and MDA-MB-468 cells were detected with qRT-PCR or western blotting. (**d–k**) The proliferation, colony formation, cell cycle progression, apoptosis, migration, and invasion of MCF-7 and MDA-MB-468 cells were assessed through CCK-8, colony formation, flow cytometry, or transwell assays. The experiments were repeated three times. Data are shown as mean ± standard deviation. *$P < 0.05$. (**a**) ( ) miR-NC, ( ) miR-326, ( ) miR-326+pcDNA-NC, and ( ) miR-326 + pcDNA-FGFR1. (**c**) ( ) miR-NC, ( ) miR-326, ( ) miR-326 + pcDNA-NC, and ( ) miR-326 + pcDNA-FGFR1. (**d**) MCF-7 (—●—) miR-NC, (—■—) miR-326, (—▲—) miR-326 + pcDNA-NC, and (—▼—) miR-326 + pcDNA-FGFR1. (**e**) MDA-MB-468 (—●—) miR-NC, (—■—) miR-326, (—▲—) miR-326 + pcDNA-NC, and (—▼—) miR-326 + pcDNA-FGFR1. (**f**) ( ) miR-NC, ( ) miR-326, ( ) miR-326 + pcDNA-NC, and ( ) miR-326 + pcDNA-FGFR1. (**g**) MCF-7 ( ) miR-NC, ( ) miR-326, ( ) miR-326 + pcDNA-NC, and ( ) miR-326 + pcDNA-FGFR1. (**h**) MDA-MB-468 ( ) miR-NC, ( ) miR-326, ( ) miR-326 + pcDNA-NC, and ( ) miR-326 + pcDNA-FGFR1. (**i**) ( ) miR-NC, ( ) miR-326, ( ) miR-326 + pcDNA-NC, and ( ) miR-326 + pcDNA-FGFR1. (**j**) ( ) miR-NC, ( ) miR-326, ( ) miR-326 + pcDNA-NC, and ( ) miR-326 + pcDNA-FGFR1. (**k**) ( ) miR-NC, ( ) miR-326, ( ) miR-326 + pcDNA-NC, and ( ) miR-326 + pcDNA-FGFR1.
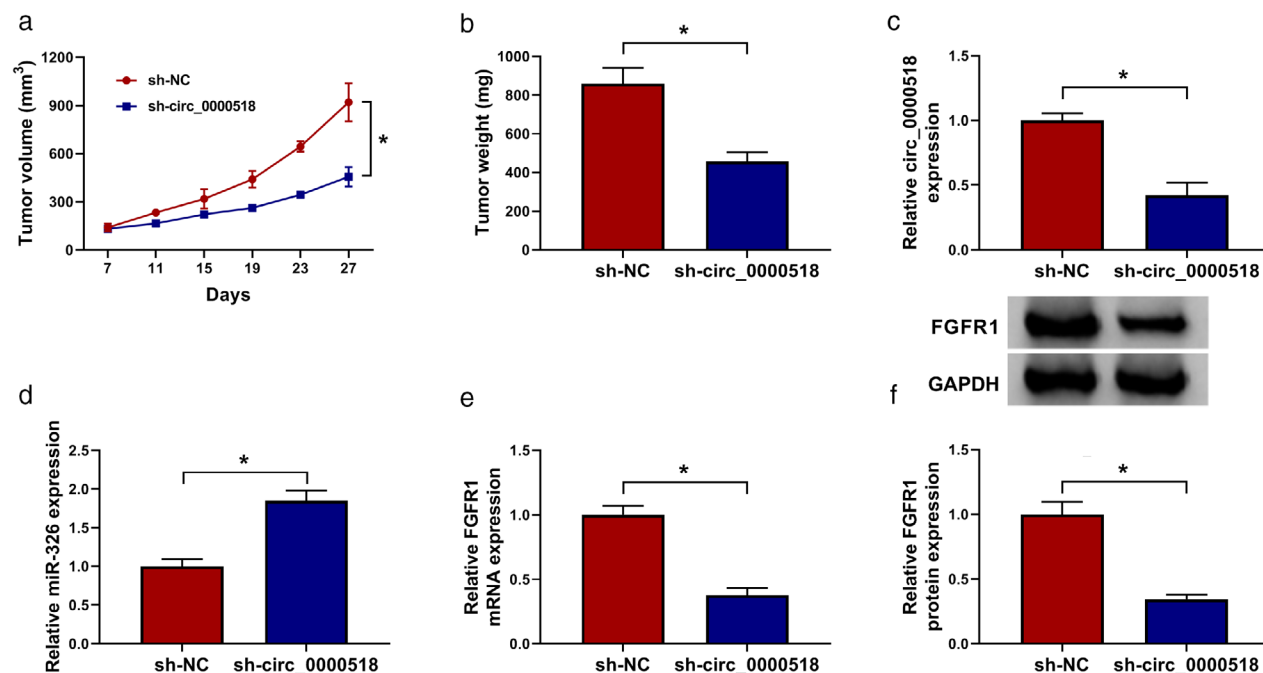
Figure 7 Circ_0000518 silencing could decrease BC growth in vivo. (**a**) The growth curves of tumor volume of the sh-circ_0000518 and sh-NC groups. (**b**) Xenograft tumor weight of the sh-circ_0000518 and sh-NC groups was assessed on day 27. (**c–f**) The levels of circ_0000518, miR-326, FGFR1 mRNA and protein in mice tumor tissues of the sh-circ_0000518 and sh-NC groups were determined with qRT-PCR or western blotting. The experiments were repeated three times. Data are shown as mean ± standard deviation. *$P < 0.05$. (**a**) (—●—) sh-NC and (—■—) sh-circ_0000518. (**b**) (■) sh-NC and (■) sh-circ_0000518. (**c**) (■) sh-NC and (■) sh-circ_0000518. (**d**) (■) sh-NC and (■) sh-circ_0000518. (**e**) (■) sh-NC and (■) sh-circ_0000518. (**f**) (■) sh-NC and (■) sh-circ_0000518.

The findings highlight the prospect of circ_0000518 as a new target for BC treatment.

Acknowledgments

Disclosure

The authors declare that there are no competing interests associated with the manuscript.

References

1 Roulot A, Héquet D, Guinebretière J-M *et al.* Tumoral heterogeneity of breast cancer. *Ann Biol Clin* 2016; **74**: 653–60.

2 Bray F, Ferlay J, Soerjomataram I, Siegel RL, Torre LA, Jemal A. Global cancer statistics 2018: GLOBOCAN estimates of incidence and mortality worldwide for 36 cancers in 185 countries. *CA Cancer J Clin* 2018; **68**: 394–424.

3 Wang H, Xiao Y, Wu L, Ma D. Comprehensive circular RNA profiling reveals the regulatory role of the circRNA-000911/miR-449a pathway in breast carcinogenesis. *Int J Oncol* 2018; **52**: 743–54.

4 Rodgers RJ, Reid GD, Koch J *et al.* The safety and efficacy of controlled ovarian hyperstimulation for fertility preservation in women with early breast cancer: A systematic review. *Hum Reprod* 2017; **32**: 1033–45.

5 Harjes U. Breast cancer: Staying silent. *Nat Rev Cancer* 2018; **18**: 136.

6 Chen LL. The biogenesis and emerging roles of circular RNAs. *Nat Rev Mol Cell Biol* 2016; **17**: 205–11.

7 Qu S, Yang X, Li X *et al.* Circular RNA: A new star of noncoding RNAs. *Cancer Lett* 2015; **365**: 141–8.

8 Li D, Yang Y, Li ZQ, Li LC, Zhu X-H. Circular RNAs: From biogenesis and function to diseases. *Chin Med J (Engl)* 2019; **132**: 2457–64.

9 Verduci L, Strano S, Yarden Y, Blandino G. The circRNA-microRNA code: Emerging implications for cancer diagnosis and treatment. *Mol Oncol* 2019; **13**: 669–80.

10 Xia T, Pan Z, Zhang J. CircSMC3 regulates gastric cancer tumorigenesis by targeting miR-4720-3p/TJP1 axis. *Cancer Med* 2020; **9**: 4299–309.

11 Lu TX, Rothenberg ME. MicroRNA. *J Allergy Clin Immunol* 2018; **141**: 1202–7.

12 Shin VY, Chu KM. MiRNA as potential biomarkers and therapeutic targets for gastric cancer. *World J Gastroenterol* 2014; **20**: 10432–9.

13 Pan YJ, Wan J, Wang CB. MiR-326: Promising biomarker for cancer. *Cancer Manag Res* 2019; **11**: 10411–8.

14 Nie FR, Li QX, Wei HF, Ma Y. miR-326 inhibits the progression of papillary thyroid carcinoma by targeting MAPK1 and ERBB4. *Neoplasma* 2020; **67**: 604–13.

15 Tao D, Zhang Z, Liu X *et al.* LncRNA HOTAIR promotes the invasion and metastasis of oral squamous cell carcinoma through metastasis-associated gene 2. *Mol Carcinog* 2020; **59**: 353–64.

16 Mossahebi-Mohammadi M, Quan M, Zhang J-S, Li X. FGF signaling pathway: A key regulator of stem cell pluripotency. *Front Cell Dev Biol* 2020; **8**: 79.

17 Shimizu D, Saito T, Ito S *et al.* Overexpression of promotes peritoneal dissemination epithelial-to-mesenchymal transition in gastric cancer. *Cancer Genomics Proteomics* 2018; **15**: 313–20.

18 Wang K, Ji W, Yu Y *et al.* FGFR1-ERK1/2-SOX2 axis promotes cell proliferation, epithelial-mesenchymal transition, and metastasis in FGFR1-amplified lung cancer. *Oncogene* 2018; **37**: 5340–54.

19 Wang W, Meng Y, Dong B *et al.* A versatile tumor gene deletion system reveals a crucial role for FGFR1 in breast cancer metastasis. *Neoplasia* 2017; **19**: 421–8.

20 Tang Q, Hann SS. Biological roles and mechanisms of circular RNA in human cancers. *Onco Targets Ther* 2020; **13**: 2067–92.

21 Tran AM, Chalbatani GM, Berland L *et al.* A new world of biomarkers and therapeutics for female reproductive system and breast cancers: Circular RNAs. *Front Cell Dev Biol* 2020; **8**: 50.

22 Liang Y, Song X, Li Y *et al.* circKDM4C suppresses tumor progression and attenuates doxorubicin resistance by regulating miR-548p/PBLD axis in breast cancer. *Oncogene* 2019; **38**: 6850–66.

23 Liu P, Zou Y, Li X *et al.* circGNB1 facilitates triple-negative breast cancer progression by regulating miR-141-5p-IGF1R axis. *Front Genet* 2020; **11**: 193.

24 Pan G, Mao A, Liu J, Lu J, Ding J, Liu W. Circular RNA hsa_circ_0061825 (circ-TFF1) contributes to breast cancer progression through targeting miR-326/TFF1 signalling. *Cell Prolif* 2020; **53**: e12720.

25 Zhao B, Song X, Guan H. CircACAP2 promotes breast cancer proliferation and metastasis by targeting miR-29a/b-3p-COL5A1 axis. *Life Sci* 2020; **244**: 117179.

26 Zheng X, Huang M, Xing L *et al.* The circRNA circSEPT9 mediated by E2F1 and EIF4A3 facilitates the carcinogenesis and development of triple-negative breast cancer. *Mol Cancer* 2020; **19**: 73.

27 Ji S, Zhang B, Kong Y, Ma F, Hua Y. miR-326 inhibits gastric cancer cell growth through downregulating NOB1. *Oncol Res* 2017; **25**: 853–61.

28 Chen Y, Wu H, Pan S *et al.* HOTAIR/miR-326/FUT6 axis facilitates colorectal cancer progression through regulating fucosylation of CD44 via PI3K/AKT/mTOR pathway. *J Cell Physiol* 2019; **1866**: 750–60.

29 Jiang H, Liang M, Jiang Y *et al.* The lncRNA TDRG1 promotes cell proliferation, migration and invasion by targeting miR-326 to regulate MAPK1 expression in cervical cancer. *Cancer Cell Int* 2019; **19**: 152.

30 Wei LQ, Li L, Lu C, Liu J. Involvement of H19/miR-326 axis in hepatocellular carcinoma development through modulating TWIST1. *J Cell Physiol* 2019; **234**: 5153–62.

31 Ghaemi Z, Soltani BM, Mowla SJ. MicroRNA-326 functions as a tumor suppressor in breast cancer by targeting ErbB/PI3K signaling pathway. *Front Oncol* 2019; **9**: 653.

32 Du Y, Shen L, Zhang W *et al.* Functional analyses of microRNA-326 in breast cancer development. *Biosci Rep* 2019; **39**: BSR20190787.

33 Liang Z, Wu H, Xia J *et al.* Involvement of miR-326 in chemotherapy resistance of breast cancer through modulating expression of multidrug resistance-associated protein 1. *Biochem Pharmacol* 2010; **79**: 817–24.

34 Chen Z, Tong LJ, Tang BY *et al.* C11, a novel fibroblast growth factor receptor 1 (FGFR1) inhibitor, suppresses breast cancer metastasis and angiogenesis. *Acta Pharmacol Sin* 2019; **40**: 823–32.

35 Turner N, Pearson A, Sharpe R *et al.* FGFR1 amplification drives endocrine therapy resistance and is a therapeutic target in breast cancer. *Cancer Res* 2010; **70**: 2085–94.

36 Ma F, Zhang L, Ma L, Zhang Y, Zhang J, Guo B. MiR-361-5p inhibits glycolytic metabolism, proliferation and invasion of breast cancer by targeting FGFR1 and MMP-1. *J Exp Clin Cancer Res* 2017; **36**: 158.

37 Golfmann K, Meder L, Koker M *et al.* Synergistic anti-angiogenic treatment effects by dual FGFR1 and VEGFR1 inhibition in FGFR1-amplified breast cancer. *Oncogene* 2018; **37**: 5682–93.

Supporting Information

Additional Supporting Informationmay be found in the online version of this article at the publisher's website:

Figure S1 Expression of five circRNAs in BC tissues. QRT-PCR revealed the expression of hsa_circRNA_001846, hsa_circRNA_000518, hsa_circRNA_002172, hsa_circRNA_002144, and hsa_circRNA_000166 in BC tissues (10 random samples) and paired para-carcinoma tissues. The experiments were repeated three times. Data were exhibited as mean $\pm$ standard deviation. $*P < 0.05$.

Figure S2 Influence of circ_0000518 overexpression on the malignant behaviors of BC cells. (**A**) QRT-PCR revealed the overexpression efficiency of circ_0000518 in MCF-7 and MDA-MB-468 cells. (**B–I**) Effects of circ_0000518 overexpression on proliferation, colony formation, cell cycle progression, apoptosis, migration, and invasion of MCF-7 and MDA-MB-468 cells were determined using CCK-8, colony formation, flow cytometry, or transwell assays. The experiments were repeated three times. Data were exhibited as mean $\pm$ standard deviation. $*P < 0.05$.